RECENT PROGRESS ON LASER PLASMA ACCELERATORS AND APPLICATIONS FOR COMPACT HIGH-QUALITY PARTICLE BEAM AND RADIATION SOURCES

K. Nakajima

High Energy Accelerator Research Organization, 1-1 Oho, Tsukuba, Ibaraki 305-0081 Japan; Shanghai Jiao Tong University, 800 Dongchuan Rd., Shanghai 200240, P. R. China
E-mail: nakajima@post.kek.jp

Recent progress in laser-driven plasma-based electron accelerators is overviewed in theoretical and experimental aspects. In particular, basic acceleration physics called as a bubble mechanism is highlighted to show recent achievements of laser plasma accelerator technologies that produce high-energy, high-quality stable beams required for compact particle beam and radiation sources.
PACS: 41.75Jv, 52.38kd, 52.50Jm

1. INTRODUCTION

In this decade, worldwide experimental and theoretical researches on laser-plasma accelerators have brought about great progress in high-energy high-quality electron beams of the order of GeV-class energy and a few % energy spread [1-6]. These high-energy high-quality particle beams make it possible to open the door for a wide range of applications in research, and medical and industrial uses.

Here recent progress in laser-driven plasma particle accelerators is overviewed in terms of particle beam parameters such as energy, energy spread, emittance, bunch length and charge, strictly determined by acceleration mechanism such as the bubble mechanism in electron acceleration.

Although there is no practical application to date, developed are various applications of laser plasma accelerators such as a compact THz or coherent X-ray radiation source and radiation therapy driven by laser-accelerated electrons [7]. On the other hand, a promising application project of laser-driven proton and ion beams to the future hadron therapy is implemented worldwide. In the future laser-plasma accelerators may come into being as a novel versatile tool for developing fields such as space science where a compact and cost-effective tool is required as well as inherent application to the energy-frontier particle accelerator.

2. LASER WAKEFIELD ACCELERATOR

2.1. LINEAR WAKEFIELD ACCELERATION

In underdense plasma an ultraintense laser pulse excites a large-amplitude plasma wave with frequency $\omega_p = (4\pi e^2 n_e/m_e c^2)^{1/2}$ and electric field on the order of $\sim n_e^{1/2}$ V/cm for the electron rest mass $m_e c^2$ and plasma density n_e cm^{-3} due to the ponderomotive force expelling plasma electrons out of the laser pulse and the space charge force of immovable plasma ions restoring expelled electrons on the back of the ion column remaining behind the laser pulse. Since the phase velocity of the plasma wave is approximately equal to the group velocity of the laser pulse $v_g/c = (1- \omega_p^2/\omega_0^2)^{1/2} \sim 1$ for the laser frequency ω_0 and the accelerating field of ~ 1 GeV/cm for the plasma density ~ 10^{18} cm^{-3}, electrons trapped into the plasma wave are likely to be accelerated up to ~ 1 GeV energy in a 1 cm plasma. More accurately in the linear regime for the normalized laser intensity

$$a_0 = 0.85\left(I\lambda^2/10^{18}\,\mathrm{W cm^{-2}}\,\mu\mathrm{m}^2\right)^{1/2} \lesssim 1,$$

where I is the laser intensity and $\lambda = 2\pi c/\omega_0$ the laser wavelength, the energy gain[8] is given by

$$E = 1.3 m_e c^2 a_0^2\, n_c/n_e$$
$$\approx 35(P/\mathrm{TW})(r_0/\mu\mathrm{m})^{-2}\left(n_e/10^{18}\,\mathrm{cm^{-3}}\right)^{-1} \quad \mathrm{GeV},$$

for the peak laser power P TW focused onto the spot radius r_0 μm, assuming that the plasma wave is efficiently excited at $\lambda_p \sim c\tau_L$ for the pulse duration τ_L, and that electrons are accelerated over the dephasing length given by $L_{dp} \sim \lambda_p(\omega_p^2/\omega_0^2) = \lambda_p(n_c/n_e)$, where $n_c = \pi/(r_e\lambda^2) \simeq 1.115\times10^{21}$ cm^{-3} $(\lambda/\mu\mathrm{m})^{-2}$ is the cutoff density, $r_e = e^2/m_e c^2$ the classical electron radius. The accelerated electrons overrun the accelerating field toward the decelerating field beyond the dephasing length.

2.2. QUASI-MONOENERGETIC ACCELERATION IN THE BUBBLE REGIME

The leading experiments [9-11] that successfully demonstrated the production of quasi-monoenergetic electron beams with narrow energy spread have been elucidated in terms of self-injection and acceleration mechanism in the bubble regime [12,13]. In these experiments, electrons are self-injected into a nonlinear wake, referred to as a "bubble", i.e. a cavity void of plasma electrons consisting of a spherical ion column surrounded with a narrow electron sheath, formed behind the laser pulse instead of a periodic plasma wave in the linear regime. As analogous to a conventional RF cavity inside which electromagnetic energy is resonantly confined at the matched frequency to accelerate externally injected particles, inducing a current flow in a skin depth of a metal surface, plasma electrons radially expelled by the radiation pressure of the laser form a sheath with thickness of the order of the plasma skin depth c/ω_p outside the ion sphere remaining "unshielded" behind the laser pulse moving at relativistic velocity so that the cavity shape should be determined by balancing the Lorentz force of the ion sphere exerted on the electron sheath with the ponderomotive force of the laser pulse.

This estimates the bubble radius R_B matched to the laser spot radius w_0 , approximately as $k_p R_B \approx k_p w_0 \approx 2\sqrt{a_0}$, for which a best spherical shape of the bubble is created. This condition is reformulated as $a_0 \simeq 2(P/P_c)^{1/3}$, where $P_c = 17(\omega_0/\omega_p)^2$ GW is the critical power for the relativistic self-focusing [13].

The electromagnetic fields inside the bubble is obtained from the wake field potential of the ion sphere moving at the velocity v_B as

$$eE_z/(m_e c\omega_p) = -k_p\xi/2, \quad eE_r/(m_e c\omega_p) = -k_p r/2,$$

where $\xi = z - v_B t$ is the coordinate in the moving frame of the bubble and r the radial coordinate with respect to the laser propagation axis [12]. One can see that the maximum accelerating field is given by $e|E_z|_{\max} = (1/2)m_e c^2 k_p^2 R_B$ at the back of the bubble and the focusing force is acting on an electron inside the bubble. Assuming the bubble phase velocity is given by $v_B \sim v_g - v_{etch} \sim c[1-(1/2+1)(\omega_p/\omega_0)^2]$, where $v_{etch} \sim c(\omega_p/\omega_0)^2$ is the velocity at which the laser front etches back due to the local pump depletion, the dephasing length leads to

$$L_{dp} \sim c/(c - v_B)R_B \sim (2/3)(\omega_0/\omega_p)^2 R_B = (2/3)(n_c/n_e)R_B.$$

Hence the electron injected at the back of the bubble can be accelerated up to the energy

$$E \approx \frac{1}{2} e|E_z|_{\max} L_{dp} \approx \frac{1}{6} m_e c^2 (k_p R_B)^2 \left(\frac{\omega_0}{\omega_p}\right)^2 \approx \frac{2}{3} m_e c^2 a_0 \frac{n_c}{n_e}.$$

Using the matched bubble radius condition, the energy gain is approximately given by

$$E \approx m_e c^2 \left(\frac{P}{P_r}\right)^{1/3} \left(\frac{n_c}{n_e}\right)^{2/3},$$

where $P_r = m_e^2 c^5/e^2 = 8.72$ GW [14].

The 2D or 3D particle-in-cell simulations confirm that quasi-monoenergetic electron beams are produced due to self-injection of plasma electrons at the back of the bubble from the electron sheath outside the ion sphere as the laser intensity increases to the injection threshold. As expelled electrons flowing the sheath are initially decelerated backward in a front half of the bubble and then accelerated in a back half of it toward the propagation axis by the accelerating and focusing forces of the bubble ions, their trajectories concentrate at the back of the bubble to form a strong local density peak in the electron sheath and a spiky accelerating field. Eventually the electron is trapped into the bubble when its velocity reaches the group velocity v_g of the laser pulse. Theoretical analysis on the trapping threshold gives $k_p R_B \geq 2^{1/2}\gamma_g = (2n_c/n_e)^{1/2}$, where $\gamma_g = [1-(v_g/c)^2]^{-1/2}$ [15]. This trapping condition leads to $a_0 \geq n_c/2n_e$, while the trapping cross section $\sigma \simeq (2\pi/k_p^3 d)(\ln k_p R_B/8^{1/2})^{-1}$ [12] with the sheath width d imposes $k_p R_B \geq 2.8$, i.e. $a_0 \geq 2$ for the matched bubble radius. Once an electron bunch is trapped in the bubble, loading of trapped electrons reduces the wakefield amplitude below the trapping threshold and stops further injection. Consequently the trapped electrons undergo acceleration and bunching process within a separatrix on the phase space of the bubble wakefield. This is a simple scenario for producing high-quality monoenergetic electron beams in the bubble regime. However, in most of laser-plasma experiments aforementioned conditions and scenarios are not always fulfilled.

In the experiment for the plasma density $n_e = (1\ldots2)\times 10^{19}$ cm^{-3}, observation of the self-injection threshold on the normalized laser intensity gives $a_{th} = 3.2$ after accounting for self-focusing and self-compression that occur during laser pulse propagation in the plasma. In terms of the laser peak power $P/P_c = (\pi^2/8)a_0^2(w_0/\lambda_p)^2$, the self-injection threshold for the power $(P/P_c)_{th} \approx 12.6$ as the laser spot size reduces to the plasma wavelength due to the relativistic self-focusing [16]. In the experiment at $n_e = (3\ldots5)\times 10^{18}$ cm^{-3}, the self-injection threshold is $(P/P_c)_{th} = 3$, corresponding to $a_{th} = 1.6$ [17]. Our 2-D PIC simulations on the self-injection threshold show that for the uniform density plasma such as a gas jet or a gas cell of $n_e = (1.7\ldots5)\times 10^{18}$ cm^{-3}, the self-injection occurs at $a_0 \geq 3.6$ and for the preformed plasma channel such as discharge capillary of the plasma density $n_e = 2\times 10^{18}$ cm^{-3} with the density depth $\Delta n_{ch}/n_e = 0.3$, the threshold is $a_{th} \sim 2.8$.

2.3. CONTROLLED INJECTIONS

For many applications of laser wakefield accelerators, stability and controllability of the beam performance such as the energy, the energy spread, the emittance and the charge are indispensable as well as compact and robust features of the system. In contrast to the conventional accelerators composed of various complex-functioned systems, the performance of laser plasma accelerators is strongly correlated to the injection mechanism of electron beams as well as the laser performance. To date, the external injection into laser wakefields from the conventional RF injector [18] or the staging concept, which is conceivable on the analogy of the high-energy RF accelerators, has not been always successful for generating intense high-quality electron beams that could be useful for applications. Hence, besides the self-injection, the optical injection scheme with two colliding pulses and the enhanced self-injection by ionization are highlighted.

The optical injection scheme for manipulating electron beams in a phase space of laser wakefield acceleration with fs-synchronization and MeV-energy response utilize an injection pulse split from the same drive pulse with fs duration, crossing the drive pulse at some angle in the plasma. When crossing each other, the phase space of wakefields excited by the drive pulse overlaps with the phase space of beat waves generated by mixing the drive pulse and the injection pulse. As a result, the ponderomotive force of the beat wave boosts plasma electrons and locally injects them into the separatrix of the wakefields. In the case of head-on collision of two counter-propagating laser pulses at the angle of 180°, the ponderomotive force $F_{bw} \simeq (1/\gamma)m_e c^2 k_0 a_0 a_1 \sin(2k_0 x)$ of the injection beat wave oscillating with the wavelength $\lambda_0/2$ locally accelerates the plasma electrons to be injected into the wakefield bucket, where $k_0 = 2\pi/\lambda_0$ is the laser wave number, a_0, and a_1 the intensity of the drive pulse and the injection pulse, respectively, and γ the Lorentz factor of the plasma electron, i.e. $\gamma \sim 1$ for the cold plasma. On the contrary to the self-injection with a single drive pulse, this force is independently controllable by changing the

injection pulse intensity and/or its polarization with respect to that of the drive pulse as well as the injection position, where two pulses collides. Therefore the energy and the charge can be controlled within some extent, associating with evolution of the energy spread due to the beam loading and the injection volume of the phase space.

These effects are successfully demonstrated with good stability by the experiments carried out below the self-injection threshold of the drive pulse intensity. The experiment of [19] with $a_0 = 1.3$, $a_1 = 0.4$ and the pulse duration of 30 fs for both pulses shows an almost linear control of the monoenergetic beam energy from 50 MeV to 250 MeV by changing the colliding position over the 2-mm gas jet at the plasma density of $n_e = 7.5 \times 10^{18}$ cm^{-3}, consequently changing the acceleration length in the average accelerating field of E_z = 270 GV/m, which is close to an estimate of the wave breaking field for the cold plasma, $E_{wb} \approx 0.96 n_e^{1/2} \sim 263$ GV/m. The experiment of [20] demonstrates the colliding optical injection at the crossing angle of 135°in the 1-mm gas jet with $a_0 = 0.6$ (P_{drive} = 3 TW), $a_1 = 0.1$ (P_{inj} = 0.14 TW) and 70 fs pulse duration, resulting in the energy E =15 MeV and the energy spread $\Delta E/E$ =7.8% at $n_e = 3.95 \times 10^{19}$ cm^{-3} free from the self-injection as well as the head-on colliding injection at 180° with $a_0 = 1.2$ (P_{drive} = 10 TW), $a_1 = 0.2$ (P_{inj} = 0.6 TW) and 40 fs pulse duration, resulting in the energy E =134 MeV and the energy spread $\Delta E/E$ =3.5% at n_e=1 × 10^{19} cm^{-3}. These experiments suggest a very compact system of the electron beam source including the laser and the accelerator on a table-top size with high quality and high stability.

2.4. IONIZATION INDUCED TRAPPING

A technique for controlling the injection into a tiny phase volume of the bubble is based on the use of chemical structure of plasma species, i.e. a mixture of gases with the different ionization potential rather than a uniform plasma of a single species. A mechanism of the ionization-induced trapping is elucidated by the fact that likely trapped are a number of electrons that are produced from impurity of gas with a large difference of the ionization potential between the outer shell electrons and the inner shell ones such as nitrogen, of which two *K*-shell electrons are ionized by the optical field ionization over the threshold intensity $I_{BS} \approx 10^{19}$ W/cm^2 (the ionization potential of 552 eV for N^{6+} and the ionization potential of 667 eV for N^{7+}), whereas *L*-shell electrons are ionized below the intensity of $I_{BS} < 10^{17}$ W/cm^2 (the ionization potential of 98 eV for N^{5+}) and can be considered preionized in the leading front of the laser pulse before the bubble formation. Hence the inner shell electrons are produced only near the peak intensity of the laser pulse, which is located near the bubble centre on the propagation axis, where the wake potential is a maximum and the expelling ponderomotive force of the laser pulse is a minimum. Contrary to preionized free electrons, whose trajectories move along a narrow sheath with radius R_B outside the bubble, the ionized electrons emitted from the inner shell move close to the bubble axis toward the back of the bubble where the wake potential is a minimum and are eventually trapped into the wakefield when electrons gain a sufficient kinetic energy required for trapping. This mechanism occurs at as the low intensity as the optical field ionization threshold for the inner shell electrons of impurity gas and significantly increases the trapped charge. As trapping occurs close to the bubble axis, amplitudes of the betatron oscillation after trapping decrease compared to the self-injection from the electron sheath. Recent experiments [21,22] support the ionization induced trapping mechanism that reduces the self-injection threshold to $P/P_c \sim 1.4$ ($a_0 \sim 1.6$) for $n_e \sim 1.4 \times 10^{19}$ cm^{-3}, 9:1 He:N_2 gas mixture, increases 4~5 times the charge for $n_e \sim 2 \times 10^{19}$ cm^{-3}, 1.2% N_2 98.8% He gas mixture with the 30 TW, 30 fs laser pulse, and produces significantly collimated electron beams. Evidence of the ionization induced electron trapping has been observed in the laser plasma acceleration experiments with ablative capillary made of acrylic resin with length of 4 cm and the capillary diameter of 500 μm. The experiment of ref. [3] shows the production of electron beams of 560 MeV for 24 TW ($a_0 \sim 1.7$), $n_e \approx 1.9 \times 10^{18}$ cm^{-3} and 190 MeV for P = 16 TW ($a_0 \sim 1.4$), $n_e \approx 2.7 \times 10^{18}$ cm^{-3}, respectively. In the experiment with the 3 cm capillary made of polyethylene with the diameter of 400 μm, however, no electron has been produced at 35 TW ($a_0 \sim 1.6$), $n_e \approx (1\ldots3) \times 10^{18}$ cm^{-3} [23]. This fact suggests that for the acrylic resin composed of C:O:H = 4:2:7 ($CH_2COOC_2H_5$) the injection is assisted by the ionization induced trapping for the outer shell electrons of oxygen, whereas for the polyethylene composed of C:O:H =1:0:2 (-$[CH_2]_n$-) the injection depends only on the self-injection of free electrons ionized by the capillary discharge and/or the optical field of the laser pulse because of no oxygen.

2.5. BEAM LOADING EFFECTS

The trapped electrons inside the bubble generate electromagnetic fields and modify the bubble wakefields. As a result, the trailing electron bunch undergoes less accelerated field that limits the charge and produces energy spread. A thorough measurement of the beam loading has been made by the use of the colliding optical injection with the pump pulse intensity a_0 = 1.5, varying the injection pulse intensity from a_1 = 0.1 to 0.4 to control the injected charge. As a result of analyzing the measured energy shift consisting of the beam loading and the injection volume effects, the beam loading field per charge is deduced as 0.8 (GV/m)/pC at $n_e \approx 5.7 \times$ × 10^{18} cm^{-3}[24]. The analysis of the beam loading in the bubble regime gives the energy absorbed per unit length of the beam is given as

$$\frac{Q_s}{1\text{nC}} \frac{eE_s}{m_e c \omega_p} \approx 0.047 \sqrt{\frac{10^{16}\,\text{cm}^{-3}}{n_e}} (k_p R_B)^4,$$

where Q_s is the total charge and E_s the accelerating wakefield at the phase position where the bunch charge starts, assuming the density distribution of the bunch charge has a trapezoidal shape so that the energy spread inside the bunch is minimized [25]. This equation implies

the trade-off between the total charge that can be accelerated and the accelerating gradient, i.e. the accelerated energy. With $k_p R_B \simeq 2\, a_0^{1/2}$, the charge is proportional to $1/n_e^{1/2}$.

Recent experiments on laser plasma acceleration successfully demonstrated GeV-class quasimonoenergetic electron beams from laser wakefield accelerators by the use of a cm-scale gas jet or a capillary plasma waveguide. Table 1 summarizes the parameters of GeV-class electron beams and the experimental condition on the laser and the plasma demonstrated by the recent laser plasma experiments.

Table 1. Recent GeV-class laser wakefield acceleration experiment

Laser and plasma	Electron beam	Ref.
P = 40 TW, τ = 37 fs a_0 = 1.4 n_e = 4.3×10^{18} cm^{-3} 33 mm gas-fill capillary	E = 1 GeV $\Delta E/E$ = 2.5 % (rms) Divergence = 1.6 mrad Charge = 35 pC	[1]
P = 18 TW, τ = 42 fs a_0 = 0.84 n_e = 8.4×10^{18} cm^{-3} 15 mm gas-fill capillary	E = 0.5 GeV $\Delta E/E$ = 2.5 % (FWHM) Divergence = 0.3 mrad Charge > 0.3 pC	[2]
P = 24 TW, τ = 27 fs a_0 = 1.7 n_e = 1.9×10^{18} cm^{-3} 4 cm ablative capillary	E = 0.56 GeV $\Delta E/E$ = 2.5 % (rms) Divergence = 1.6 mrad Charge > 10 fC	[3]
P = 32 TW, τ = 80 fs a_0 = 0.8 n_e = 1.8×10^{18} cm^{-3} 3 cm gas-fill capillary	E = 0.52 GeV $\Delta E/E$ = 5 % (FWHM) Divergence = 5.4 mrad Charge = 70 pC	[4]
P = 180 TW, τ = 55 fs a_0 = 3.9 n_e = 5.7×10^{18} cm^{-3} 8 mm gas jet	E = 0.8 GeV $\Delta E/E$ = 12 % (FWHM) Divergence = 3.6 mrad Charge = 90 pC av.	[5]
P = 65 TW, τ = 60 fs a_0 = 2.8 n_e = 3×10^{18} cm^{-3} 8 mm gas jet	E = 0.72 GeV $\Delta E/E$ = 14 % (FWHM) Divergence = 2.9 mrad Charge = 100 pC	[6]

3. APPLICATIONS TOWARD TABLE-TOP SOFT X-RAY FEL

It is prospectively conceivable that a compact source producing high-energy high-quality electron beams from laser plasma accelerators are an essential tool for many applications, such as THz and X-ray synchrotron radiation sources and a unique medical therapy as well as inherent high-energy accelerators for basic sciences. In particular the present achievements of the laser wakefield accelerator performance on the beam properties such as the GeV-class energy, the 1%-level energy spread, a few πmm-mrad emittance, the 100 pC-level charge and a few fs bunch length, and good stability and controllability of the beam production allow us to downsize a large-scale X-ray synchrotron radiation source and FEL to a table-top scale including laser drivers and radiation shields as shown in the Figure. The undulator radiation from laser-plasma accelerated electron beams are first demonstrated at the wavelength of λ_{rad} = 740 nm and the estimated peak brilliance of the order of 6.5×10^{16} photons/s/mrad^2/mm^2 /0.1% bandwidth driven by the electron beam from a 2-mm-gas jet with E = 64 MeV, $\Delta E/E$ = 5.5% (FWHM) and total charge 28 pC [26]. The soft X-ray undulator radiation is successfully demonstrated at the wavelength λ_{rad} = 18 nm and the estimated peak brilliance of the order of ~ 1.3×10^{17} photons/s/mrad^2/mm^2/0.1% bandwidth radiated by electrons with E = 207 MeV, $\Delta E/E$ = 6% (FWHM) and total charge 30 pC from a 15-mm-hydrogen-fill gas cell driven by the 20 TW 37 fs laser pulse at the plasma density n_e = 8×10^{18} cm^{-3} [27]. These experiments show the tunability of the radiation wavelength with respect to the electron beam energy $\gamma = E/m_e c^2$ as $\lambda_{rad} = (\lambda_u/2h\gamma^2)(1+(K^2/2))$, where λ_u is the undulator period, h the harmonic order and $K = 0.93\lambda_u[\mathrm{cm}]B_0[\mathrm{T}]$ the undulator parameter with the magnetic field B_0.

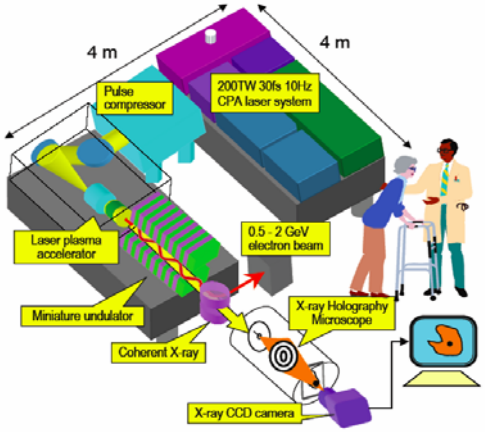

A concept of table-top soft X-ray FEL

Table 2. A design of table-top soft X-ray FEL

ELECTRON BEAM PARAMETERS	
Beam energy	E_b = 243 MeV
Peak beam current	I_b = 10 kA
energy spread (rms)	σ_E/E_b = 0.4%
Pulse duration	τ_b = 10fs
Normalized emittance	ε_n = 7 πmm mrad
UNDULATOR PARAMETERS	
Undulator period	λ_u = 5 mm
Strength parameter	K = 0.465
Undulatot length	L_u = 1.1 m
X-RAY PARAMETERS	
Wavelength	λ_{rad} = 13.5 nm (E_x = 92 eV)
FEL saturation power	P_x = 10 GW

With extremely small energy spread and peak current high enough to generate self-amplified spontaneous emission so-called SASE, a photon flux of the undulator radiation could be amplified by several orders of magnitude to levels of brilliance similar to current large-scale X-ray FELs [28]. As an example, a design of the table-top soft X-ray FEL is shown in Table 2. In order to show feasibility of this soft X-ray FEL, we made the 2D PIC simulation of a capillary laser wakefield accelerator

with the laser intensity $a_0 = 2$, the spot radius $r_0 = 20$ μm, the plasma density $n_e=2\times10^{18}$ cm^{-3}, the channel density depth $\Delta n_{ch}/n_e = 0.3$, and the pulse duration $\tau_L = 38$ fs. The simulation results show the electron beam energy E_b = 260 MeV, the rms energy spread σ_E/E_b = 0.5%, the normalized emittance $\varepsilon_n = 2.1$ πmm mrad, the pulse duration $\tau_b \sim 1.9$ fs and the peak current I_b=10.5 kA. These electron beam parameters indicate a distinct possibility of the table-top soft X-ray FEL with the capillary laser wakefield accelerator driven by 54 TW laser and a 1.1-m long undulator with 5-mm period and the 1-Tesla magnetic field.

CONCLUSIONS

Recent progress and achievements in laser-plasma accelerators are overviewed from the aspects on the bubble mechanism, the self-injection, the control and the beam loading to lead accelerated-electron beams to the high-energy and high-quality performance as compact particle and radiation sources. As an example of applications, the design of the table-top soft X-ray FEL that generates coherent radiations at the wavelength of 13.5 nm is presented.

REFERENCES

1. W.P. Leemans, B. Nagler, et al.// *Nature Physics*. 2006, v. 2, p. 696.
2. S. Karsh, J. Osterhoff, et al.// *New Journal of Physics*. 2007, v. 9, p. 415.
3. T. Kameshima, W. Hong, et al.// *Applied Physics Express*. 2008, v. 1, p. 066001.
4. T.P.A. Ibbotson, N. Bourgeois et al.// *Physical Review Special Topics: Accelerators and Beams*. 2010, v. 13, p. 031301-1.
5. S. Kneip, S.R. Nagel, et al.// *Physical Review Letters*. 2009, v. 103, p. 035002.
6. D.H. Froula, C.E. Clayton, et al.// *Physical Review Letters*. 2009, v. 103, p. 215006.
7. V. Malka, J. Faure, et al.// *Nature Physics*. 2008, v. 4, p. 447.
8. K. Nakajima// *Physics of Plasmas*. 1996, v. 3, p. 2169.
9. S.P.D. Mangles, C.D. Murphy, et al.// *Nature*. 2004, v. 431, p. 535.
10. C.G.R. Geddess, Cs. Toth, et al.// *Nature*. 2004, v. 431, p. 538.
11. J. Faure, Y. Glinec, et al.// *Nature*. 2004, v. 431, p. 541.
12. I. Kostyukov, A. Pukov and S. Kiselev// *Physics of Plasmas*. 2004, v. 11, N 11, p. 5256.
13. W. Lu, C. Huang, et al.// *Physical Review Letters*. 2006, v. 96, N 16, p. 165002.
14. W. Lu, M. Tzoufras, et al.// *Physical Review Special Topics: Accelerators and Beams*. 2007, v. 10, N 6, p. 061301.
15. I. Kostyukov, E. Nerush, et al.// *Physical Review Letters*. 2009, v. 103, p. 175003.
16. S. P.D. Mangles, A.G.R. Thomas, et al.// *Physics of Plasmas*. 2007, v. 14, p. 056702.
17. D. H. Froula, C. E. Clayton, et al.// *Physical Review Letters*. 2009, v. 103, p. 215006.
18. M. Kando, H. Ahn, et al.// *Japanese Journal of Applied Physics*. 1999, v. 38, p. L967-L969.
19. J. Faure, C. Rechatin, et al.// *Nature*. 2006, v. 444, p.737.
20. H. Kotaki, I. Daito, et al.// *Physical Review Letters*. 2009, v. 103, N 19, p. 194803.
21. A. Pak, K. A. Marsh, et al.// *Physical Review Letters*. 2010, v. 104, N 2, p. 025003.
22. C. McGuffey, A.G.R. Thomas, et al.// *Physical Review Letters*. 2010, v. 104, N 2, p. 025004.
23. C. McGuffey, M. Levin, et al.// *Physics of Plasmas*. 2009, v. 16, p. 113105.
24. C. Rechatin, X. Davoine, et al.// *Physical Review Letters*. 2009, v. 103, N 19, p. 194804.
25. M. Tzoufras, W. Lu, et al.// *Physical Review Letters*. 2008, v. 101, N 14, p. 145002.
26. H.-P. Schlenvoigt, K. Haupt, et al.// *Nature Physics*. 2008, v. 4, p. 130.
27. M. Fuchs, R. Weingartner, et al.// *Nature physics*. 2009, v. 5, p. 826.
28. K. Nakajima // *Nature physics*. 2008, v. 4, p. 92.

Article received 13.09.10

НОВЫЙ ПРОГРЕСС В РАЗРАБОТКЕ ЛАЗЕРНО-ПЛАЗМЕННЫХ УСКОРИТЕЛЕЙ И ИХ ПРИМЕНЕНИИ ДЛЯ СОЗДАНИЯ КОМПАКТНЫХ ВЫСОКОКАЧЕСТВЕННЫХ ИСТОЧНИКОВ ПУЧКОВ И ИЗЛУЧЕНИЯ

К. Накаджима

Приведен обзор нынешнего прогресса в теоретических и экспериментальных исследованиях электронных ускорителей, основанных на лазерно-плазменном взаимодействии. В частности, фундаментальная физика ускорения, называемая механизмом «пузыря», выдвигается на первый план для демонстрации последних достижений лазерно-плазменных ускорительных технологий получения высококачественных стабильных пучков высокой энергии, требуемых для компактных источников пучков и излучения.

НОВИЙ ПРОГРЕС В РОЗРОБЦІ ЛАЗЕРНО-ПЛАЗМОВИХ ПРИСКОРЮВАЧІВ І ЇХ ЗАСТОСУВАННІ ДЛЯ СТВОРЕННЯ КОМПАКТНИХ ВИСОКОЯКІСНИХ ДЖЕРЕЛ ПУЧКІВ І ВИПРОМІНЮВАННЯ

К. Накаджіма

Приведено огляд нинішнього прогресу в теоретичних і експериментальних дослідженнях електронних прискорювачів, заснованих на лазерно-плазмовій взаємодії. Зокрема, фундаментальна фізика прискорення, що називається механізмом «пузиря», висувається на перший план для демонстрації останніх досягнень лазерно-плазмових прискорювальних технологій отримання високоякісних стабільних пучків високої енергії, які потребуються для компактних джерел пучків і випромінювання.